

# Modeling and Analyzing the CESR-c Lattice

L.J.Antonelli

*University of Dallas, Irving, TX, 75062*

(Dated: August 12, 2004)

Software programs were developed to study the various properties of the current CESR-c 1.8 GeV accelerator lattice. The analyses conducted fall into two main categories. First, the accelerator was examined by investigating the particle orbits. Secondly, the Twiss functions were used to observe the effects of various parameters (i.e. positron bunch current, pretzel orbit, etc.). The underlying theory for these experiments, the processes used to conduct them, and the results obtained from them will be discussed in this paper.

## I. INTRODUCTION

The Cornell Electron Storage Ring (CESR) lattice has changed frequently and dramatically since its original inception in 1979. Throughout CESR's history, physicists here at Cornell have been aided by computer simulations, mostly written in FORTRAN and using the BMAD libraries, in understanding the inner workings of the accelerator. The goal of this project was to develop such software programs and explore the properties of the CESR-c 1.8 GeV lattice currently being used. Programs were written and developed that could analyze various characteristics of the accelerator. These programs were run with a plethora of different settings, varying different parameters (such as the amplitude of the pretzel orbit and the bunch current) and observing the effects on the beam. First, the particle orbits in the horizontal and vertical directions were examined in different lattice elements and under different conditions. Secondly, the Twiss functions, specifically the beta functions, were examined in the same scenarios. Under the headings of these two topics, many specific studies were conducted, all of which, in turn, will be described in detail. Through this investigation into the nature of the current accelerator lattice, much knowledge can be gained about the properties of storage rings in general. In addition to this, undesirable resonances were located and identified, which would help those who attempt to tune the accelerator around these types of points.

## II. THEORY

The first cyclotron was built by Ernest Lawrence at Berkeley in 1929. Five years later, in 1934, the world's second cyclotron was built here at Cornell by Livingston, a student of Lawrence's. It was a simple cyclotron which could accelerate protons to 2 MeV. Since then the field of accelerator physics has grown tremendously, producing such incredibly sophisticated systems as the Large Hadron Collider (LHC) nearing completion at CERN in Geneva, Switzerland. For an in depth discussions of the theory behind such accelerators see Edwards and Syphers.[1] While Cornell's accelerator is a far cry from the LHC, it is nonetheless quite complex. The machine uses radio frequency (RF) cavities in a linear accelerator (LINAC) to accelerate electrons and positrons, at separate times, up to about

150 MeV. The particle “beam” is actually groups of particle bunches, in between which there is empty space. From the LINAC the particles are directed into the synchrotron, which further accelerates them to the energy desired for research purposes. Right now the beams are running at energies of 1.8 GeV; the energy at which bound states of charm quarks can most effectively be studied. Once the beams are at the correct energies, they are injected, in turn, into the storage ring. This is the point at which the simulations with which this project is concerned become relevant. The beams are circulated in opposite directions around the ring. They are not accelerated to any higher energies, however, they do pass through more SRF cavities to resupply the energy to the beam that it loses through synchrotron radiation. Using a pretzel orbit, the beams are made to avoid each other at all points besides the interaction point, at which they collide and produce the events studied by the high energy group. The programs written for this project only track one beam in the storage ring at a time. Which beam is tracked can be chosen, and for all runs in this study, the electron beam was tracked. Although it only tracks one beam, a set of commands was added to simulate the electromagnetic effects of the opposing beam on the beam being tracked. These interactions occur at various places around the ring, including a larger, stronger interaction at the point at which the two beams collide (also called the interaction point or IP). Both the long range beam beam interactions (LRBBI) and the interaction point beam beam interactions (IPBBI) will be discussed further in a later section.

### A. Lattice Elements

By bending a particle’s trajectory into a circular path, the particle’s vector velocity is always drastically being changed. The force needed to produce this effect is generated through the Lorentz mechanism, governed by the familiar equation:

$$\frac{d\vec{p}}{dt} = e(\vec{E} + \vec{v} \times \vec{B}) \quad (1)$$

where  $\vec{p} = \gamma m \vec{v}$ . A large  $\vec{B}$  field is applied in the direction that bends the particle trajectory towards the center of the accelerator ring. This is done with dipole magnets as shown in Fig. 1.

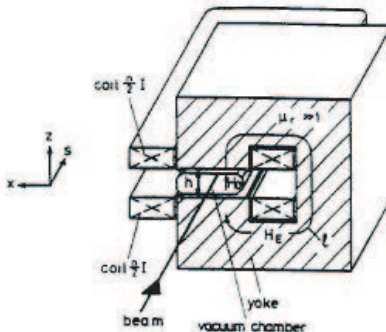


FIG. 1: Cross section of a dipole magnet

Since the magnetic field produced in a dipole:

$$\vec{B} = \frac{2\mu_0 N I}{h} \quad (2)$$

is directly proportional to  $I$ , the correct bend radius for the particles can be established simply by adjusting the current to all of the dipole magnets in the lattice. However, simply bending the particles in the proper trajectories, i.e. eliminating the path deviations, doesn't take into account a variety of other deviations. For instance, the particles in each bunch are of like charge, and they are very tightly packed together. Because of this, the Coulomb force (Eq. 3) acting to break the bunch apart is very great.

$$\vec{F} = \frac{kq_1q_2}{r^2} \quad (3)$$

Therefore, there is an obvious need for some sort of focusing device, to keep the bunch from expanding to larger than the size of the beampipe. This effect is achieved through the use of quadrupole magnets.

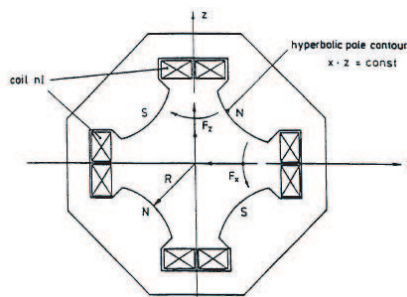


FIG. 2: Cross section of a quadrupole magnet

The effect of a quadrupole magnet can be approximated as a thin lens. The farther a particle is away from the center of the magnet, the more focusing field it encounters. Just like a thin lens, a quadrupole magnet has a characteristic focal length:

$$\frac{1}{f} = \frac{eB'l}{p} \quad (4)$$

where  $p$  is momentum,  $e$  is the electron charge,  $l$  is the length of the magnet, and  $B'$  is the gradient of the magnetic field. However, due to restrictions implied by Maxwell's equations (coming from  $\vec{\nabla} \times \vec{B} = 0$ ), the field in this type of magnet will be equally defocusing in the direction perpendicular to the focusing direction. To achieve a net focusing in both transverse directions, combinations of dipoles and alternating vertically and horizontally focusing quadrupoles are strung together. As long as the arrangement of magnets meets the stability requirement of  $\frac{L}{2f} \leq 1$ , none of the beam will be lost and the particles can circulate in a stable orbit around the accelerator. The job of designing a lattice becomes more complicated when the goal is to circulate two beams in opposite directions in the same tube at one time. Fortunately, the same configuration of magnets works for both beams because the beam traveling the opposite direction has the opposite charge and the same mass. If both beams use the same orbit directly down the center of the beampipe, they will collide everywhere around the ring instead of only at the designated interaction point equipped with a detector. Four electrostatic devices called horizontal separators kick the beams into a "pretzel orbit". This pretzel orbit allows the beams to occupy the same tube without hitting each other. Fig. 3 shows the concept of a pretzel orbit.

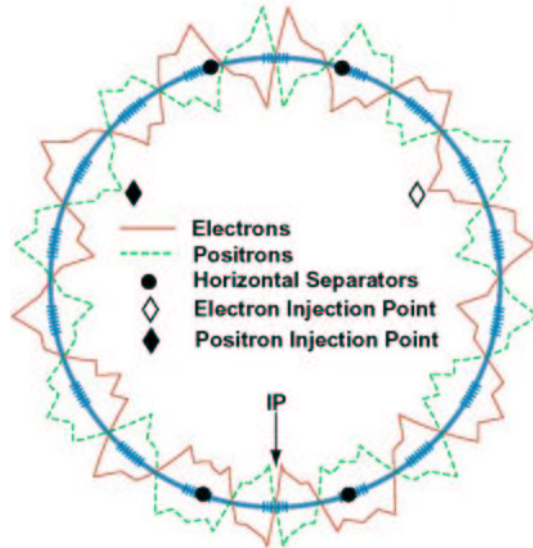


FIG. 3: Conceptual diagram of pretzel orbit in the CESR ring, along with the placements of separators and particle injection points.

The final pieces of a complete set of twelve superconducting wiggler magnets have recently been implemented in CESR. A wiggler magnet is actually a set of small magnets which are laid side to side, in an alternating North/South alignment. This is done so that the field that a particle sees as it passes through a wiggler changes direction by 180 degrees at very small intervals. This causes the particle to accelerate very quickly back and forth as it sees the opposing fields, or, in other words, it “wiggles”. The wigglers serve two purposes. The first is produce synchrotron radiation. Any charged particle being accelerated will radiate according to the Larmor formula:

$$P = \frac{1}{6\pi\epsilon_0} \frac{e^2 a^2}{c^3} \quad (5)$$

where  $P$  is the radiated power,  $e$  is the electron charge,  $a$  is the acceleration of the particle, and  $c$  is the speed of light. The radiation, in this case X-rays, is used in the Cornell High Energy Synchrotron radiation Source (CHESS) facilities to perform various types of other scientific experiments. The other utility of the wigglers is in their ability to damp out unwanted fluctuations in the particle orbits. This is especially useful in the current lattice because it is running at a smaller energy than usual. The wigglers decrease the beam energy by changing it into radiation. This speeds up the process of filling the pipe at the beginning of a run, because the second beam cannot be injected until the first beam has reached a stable orbit. Fig. 4 is a diagram of a CHESS wiggler magnet.

## B. Mathematical Descriptions

The Courant-Snyder parameters, also called the Twiss functions, are mathematical tools used to analyze the operation of an accelerator. Of the three functions ( $\alpha$ ,  $\beta$ , and  $\gamma$ ) the  $\beta$  function is the most useful for the purposes of this study. Also called the amplitude function,

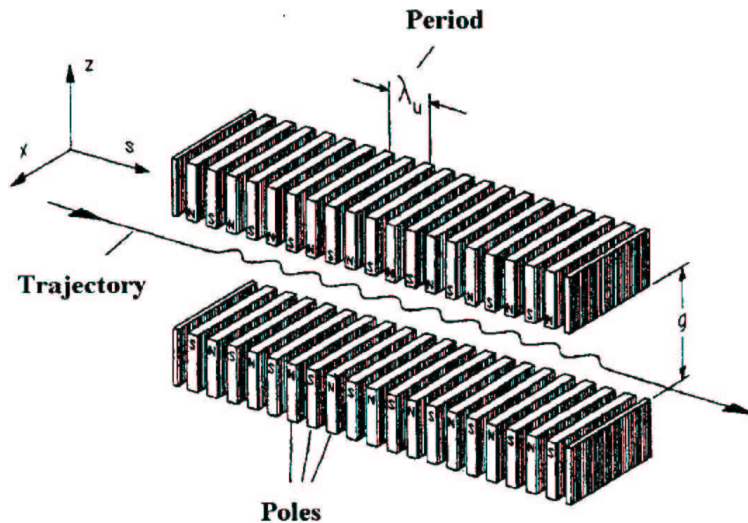


FIG. 4: Diagram of a CHESS wiggler magnet

$\beta$  is related to the overall size of the beam. The root mean squared (RMS) extent of the beam at any time can be described in terms of  $\beta$  as shown in Eq. 6:

$$\sigma_x = \sqrt{\frac{\epsilon\beta}{\pi}} \quad (6)$$

where  $\epsilon$  is the emittance of the beam. The tune of an accelerator is defined as the number of beam-function oscillations the beam makes in one turn around the ring. These oscillations can be either transverse or longitudinal. The transverse oscillations are called betatron oscillations and the longitudinal ones are called synchrotron oscillations. The tune can be looked at in two ways. First, it can be described as the fraction of the betatron (or synchrotron) oscillation frequency to the frequency of revolution, as is Eq. 7.

$$\nu \equiv \frac{f_{betatron}}{f_{revolution}} \quad (7)$$

The tune can also be calculated in terms of the integral around the ring of the  $\beta$  functions, as described in Eq. 8.

$$\nu \equiv \frac{1}{2\pi} \oint \frac{ds}{\beta(s)} \quad (8)$$

The tunes are determined by the strength of the quadrupole magnets, as well as many elements such as the sextupoles, wigglers, and even the beam-beam interactions. The lattice is *tuned* around certain undesirable values of the tunes. For instance, if the horizontal tune is an integer or a half integer, a resonance is hit and the beam will not propagate. This happens because the instabilities in the beam are not damped out, but rather amplified as the beam circulates. In other words, running at an integer transverse tune will cause to receive the same “kick” from a given element every time it goes through it. These kicks will add up constructively over multiple revolutions, and eventually kick the beam out of the pipe completely. For this reason, accelerators are operated within very small ranges of tune values.

### III. PROCEDURES

The programs that were written for this project can be divided into two categories, based on their purposes. The first type of program was used to track the particles through the accelerator and calculate all the information about the particle beam. These programs were written in FORTRAN 90, and made use of the BMAD libraries. BMAD is a set of code written at Cornell over a period of many years which models the physics of particles in accelerators.<sup>1</sup> The routines in BMAD can be combined to create programs to record virtually any piece of data from particles being circulated with virtually any set of parameters. In this project, three specific programs were used that were basically compilations of different BMAD routines. First, a program called *envelope* was used. This program was developed by S. Henderson and J. Crittenden. Its purpose is to model the injection of the second particle beam into CESR in the presence of a stored beam, and to track both beams around the ring for a given number of turns. It is mainly used to test the injection efficiency with a given set of parameters, however it can be and has been used for other purposes as well. The second program used is called *twissdisplay single*. It was originally written by J. Crittenden and developed by J. Antonelli and D. Kettler. It tracks one beam once around the ring, recording information about the beam at every point in CESR. Thirdly, the program *twissdisplay*, written and developed by J. Antonelli, was used for the same purposes as *twissdisplay single*, with one difference. *Twissdisplay* performed the same task as *twissdisplay single*, except it iterated over different parameters. For instance, it could be programmed to track the beam once around the ring for many different values of positron bunch current. This project only analyzed data that came from the last two programs, while basing its endeavors on experience gained working with *envelope*. The second type of program utilized in this project was graphing software. Programs were written in Physics Analysis Workstation (PAW) to process the data stored in *ntuple* files by the FORTRAN programs. From the graphs made by PAW, the properties of the particle beam could be analyzed as functioned of the input parameters that were changed for each particular run.

### IV. ANALYSIS/RESULTS

#### A. Orbits

The most basic piece of data examined in this study is the particle orbit itself. It was plotted in both transverse directions. Figure 5 shows the horizontal orbit as it travels once around the CESR tunnel.

This graph is basically a view looking down from above the beampipe, observing a single particle bunch traveling around the ring. It can be observed that the data stops at  $s = 76843.977\text{m}$ , which is the length of the central orbit. The red line represents the center of the beam bunch. The beam is also changing size throughout its path around the ring, but this is not shown here and will be discussed in a later section. The pretzel orbit can be observed as the center of the bunch oscillates back and forth around the center of the pipe (represented by the thin black line at  $x = 0$ ). The blue vertical lines denote the locations of the quadruple magnets. The quadruples don't have a consistent effect on the orbit, but

---

<sup>1</sup> For a list of BMAD routines, see <http://cesrelog.lns.cornell.edu/cgi/viewcvs/viewcvs.cgi/src/bmad/code/>

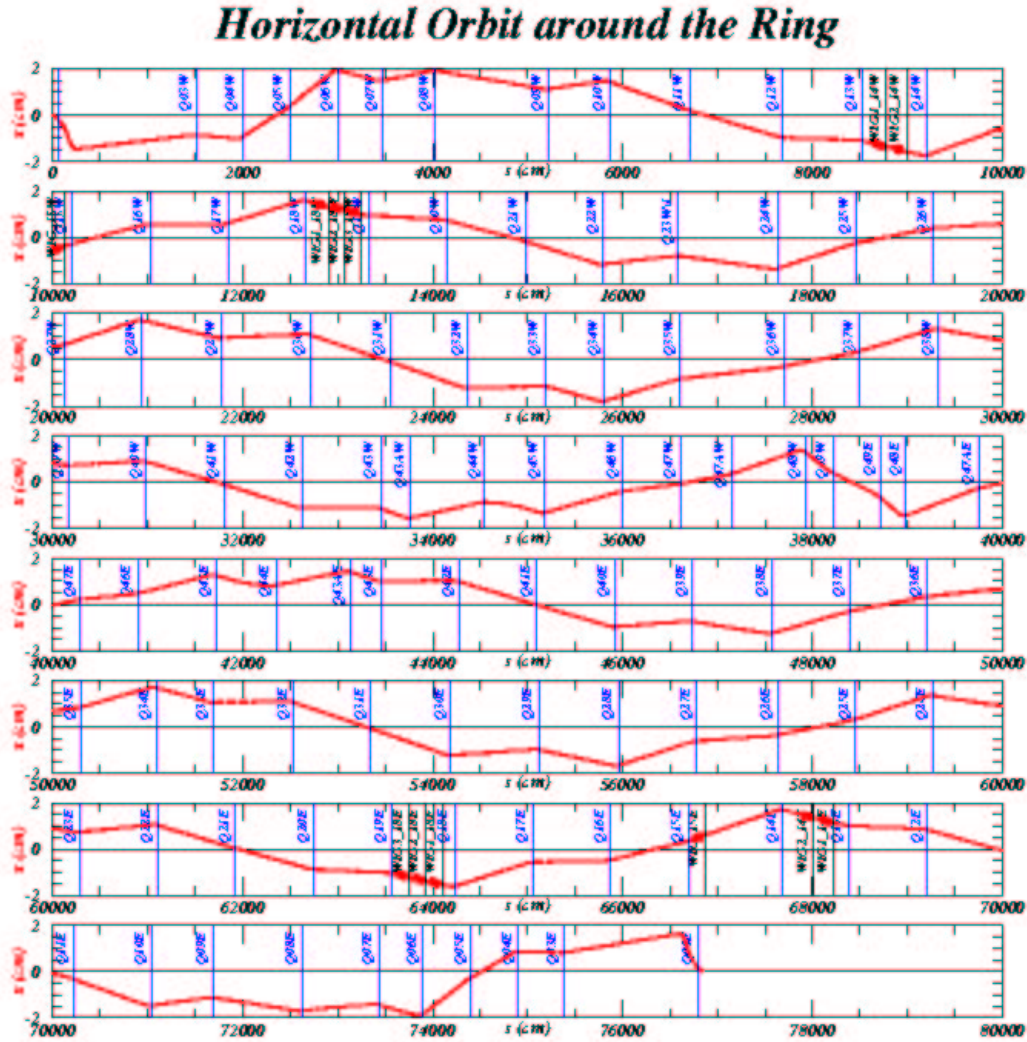


FIG. 5: Plot of the  $x$  orbit traced through one revolution around the ring, with all quadrupole and wiggler magnets labeled. The zero line represents the theoretical orbit at the center of the beam pipe.

this is because there are many other lattice elements that are unlabeled that are directing the particles. It can be seen that the bunch is centered in the pipe at the beginning and the end of the tracking. These points are where the two beams collide, so they both need to be exactly centered in order to collide most efficiently. The interaction point will be discussed in more detail in a later section. The black vertical lines denote the placement of the wiggler magnets. The oscillations caused by the wigglers can be slightly seen in this plot. A more detailed analysis of these points was conducted later in the study.

Fig. 6 shows the vertical orbit tracked once around the ring. This graph is basically the same as Fig. 5, except instead of being viewed from above the beam pipe, it is a view from the side of the pipe. Notice that while the  $x$  orbit varies by as much as 2 cm from the center of the pipe, the  $y$  orbit stays within  $150\mu\text{m}$  of the pipe center. This is true except directly before and after the interaction point, where the  $y$  orbit is kicked out to  $\sim 0.5$  cm, which

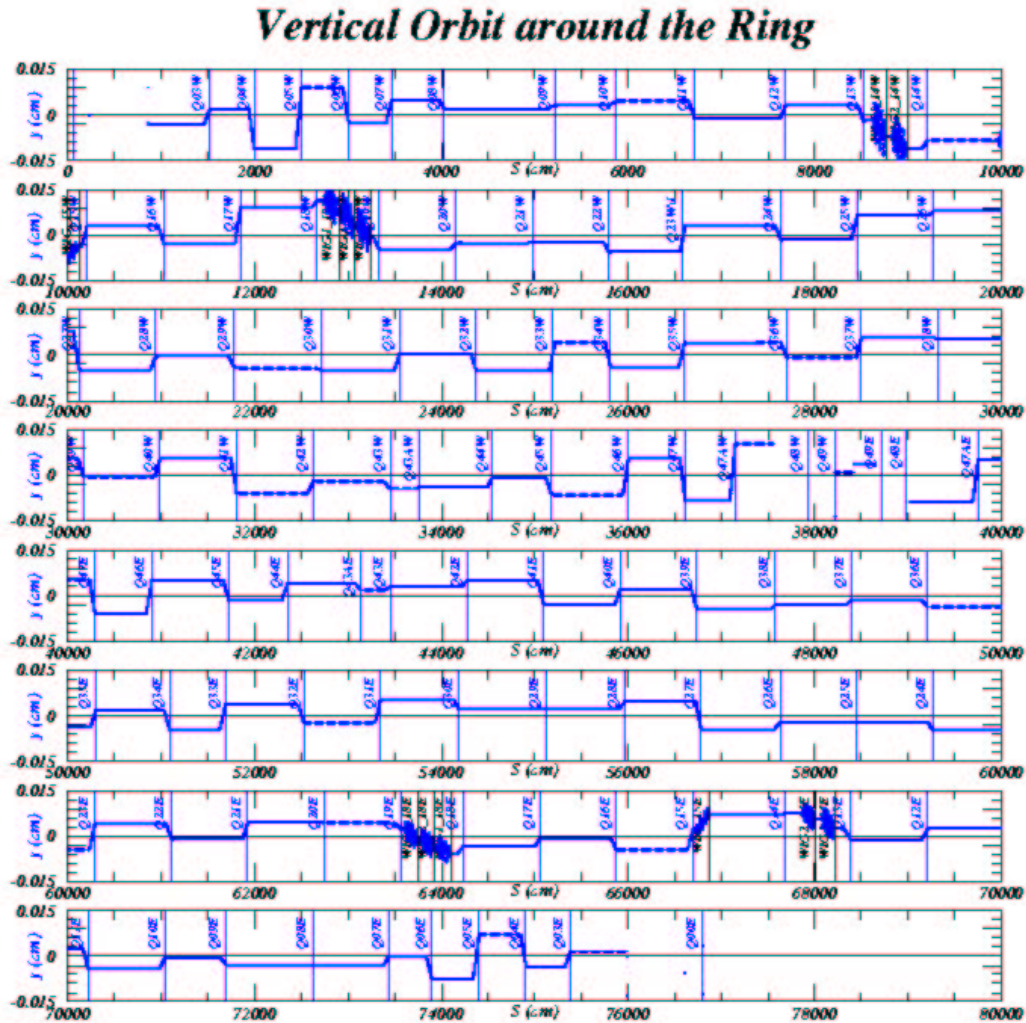


FIG. 6: Plot of the  $y$  orbit traced through one revolution around the ring, with all quadrupole and wiggler magnets labeled. The zero line represents the theoretical orbit at the center of the beampipe.

is still within the beampipe. The quadrupoles don't have the same effect on the horizontal and vertical orbits. They shift the  $y$  orbit drastically up or down. However, it's important to note that they do not affect the beam's direction, as the bunch continues straight down the pipe after exiting a quadrupole.

Fig. 7 shows a more focused plot of the orbits through 3 wiggler magnets. The physical dimensions of the wigglers can be deduced from this plot. They must be between 1 and 1.5 meters in length. The oscillations induced in the  $x$  plane are on the order of  $0.3\text{ cm}$ , while those in the  $y$  plane are at most  $100\mu\text{m}$ . It can be seen that each wiggler contains eight alternately aligned magnets. Also, one can observe that the overall particle path is not affected by the wigglers. If one connected the straight sections before and after each wiggler, they would make one straight, continuous orbit.

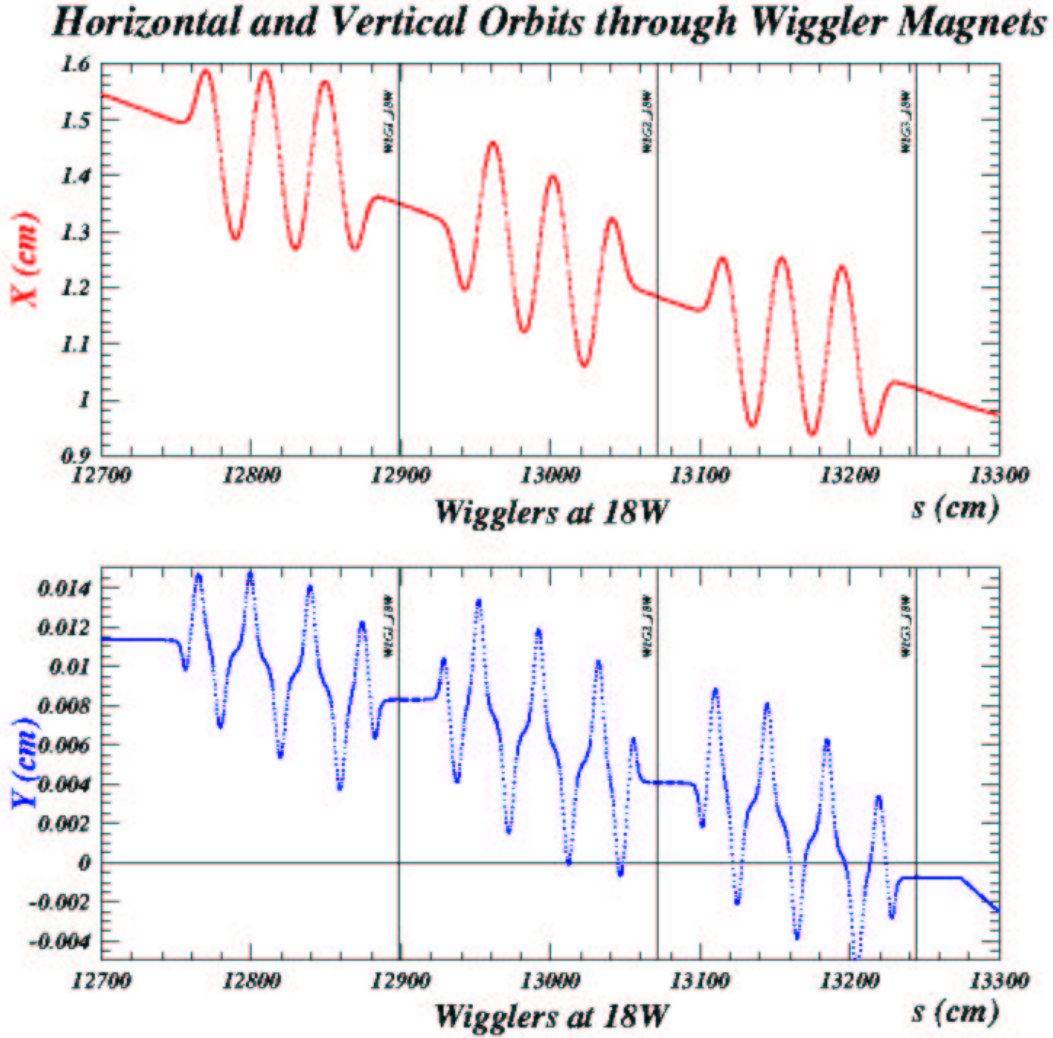


FIG. 7: Plot of the  $x$  and  $y$  orbits as they pass through the 3 wiggler magnets at position 18W.

### B. $\beta$ Functions

The second topic of analysis in this study is the  $\beta$  function, plotted, like the orbit, in both transverse directions. Both the horizontal and vertical  $\beta$  functions are plotted in Fig. 8. These functions are directly related to the RMS beam size, as described in Eq. 6, so this plot can be interpreted as the beam's size or even the beam's density, as it travels around the ring. The effect of the quadrupole magnets on the  $\beta$  functions can easily be seen. Since a quadrupole's purpose is to focus the beam, or in other words decrease its size and increase its density, we would expect the  $\beta$  functions to decrease as they pass through the quadrupoles. However, since they can only focus one transverse direction at a time, each quadrupole can be seen to increase one of the  $\beta$  functions and decrease the other. From this information, it can be deduced in which direction any given quadrupole focuses the beam. For instance, Q17W, located approximately at  $s = 110$  m, is a horizontally focusing magnet because it decreases  $\beta_x$  and increases  $\beta_y$ . We notice that higher  $\beta$ 's are deflected more in the quadrupoles. This is because, like in a thin lens, the farther a particle is from the center of the magnet, the

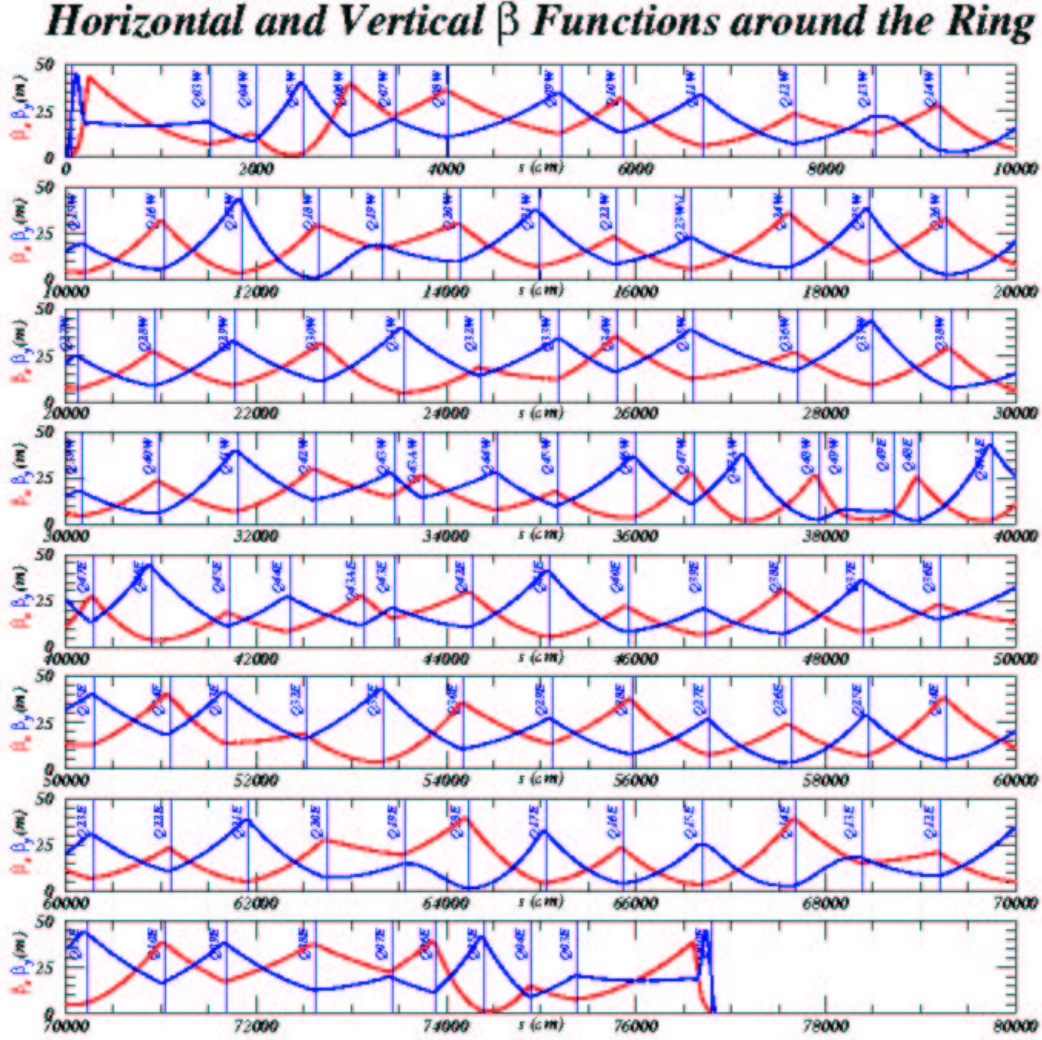


FIG. 8: Plot of  $\beta_x$  and  $\beta_y$  traced through one revolution around the ring, with all quadrupole magnets labeled.

more focusing field it is subjected to, and the more it is deflected. Combining data from Fig. 6 and Fig. 8, it can be reasoned that the direction the horizontal and vertical orbits are deflected passing through the quadrupoles is independent of which direction the quadrupole focuses. This characteristic of the orbit must be established by other lattice elements than the quadrupoles, such as the sextupole magnets. Just as in Fig. 5 and Fig. 6, the  $\beta$  functions become very small at the beginning and end of the plot, near the interaction point. This is beneficial to the collision rate at the IP, because both beams are made to be as dense as possible. More will be said about the  $\beta$  functions near the IP in a later section.

Although the effect of the wiggler magnets on the  $\beta$ 's cannot be seen as easily as their effects on the orbit, on closer inspection, more information can be gathered. Fig. 9 shows both  $\beta$  functions through the wigglers as well as the horizontal orbit for reference. Where the vertical  $\beta$  should be increasing quadratically, as it would in a dipole magnet, it increases more slowly and actually begins focusing before it enters the next quadrupole. From this it

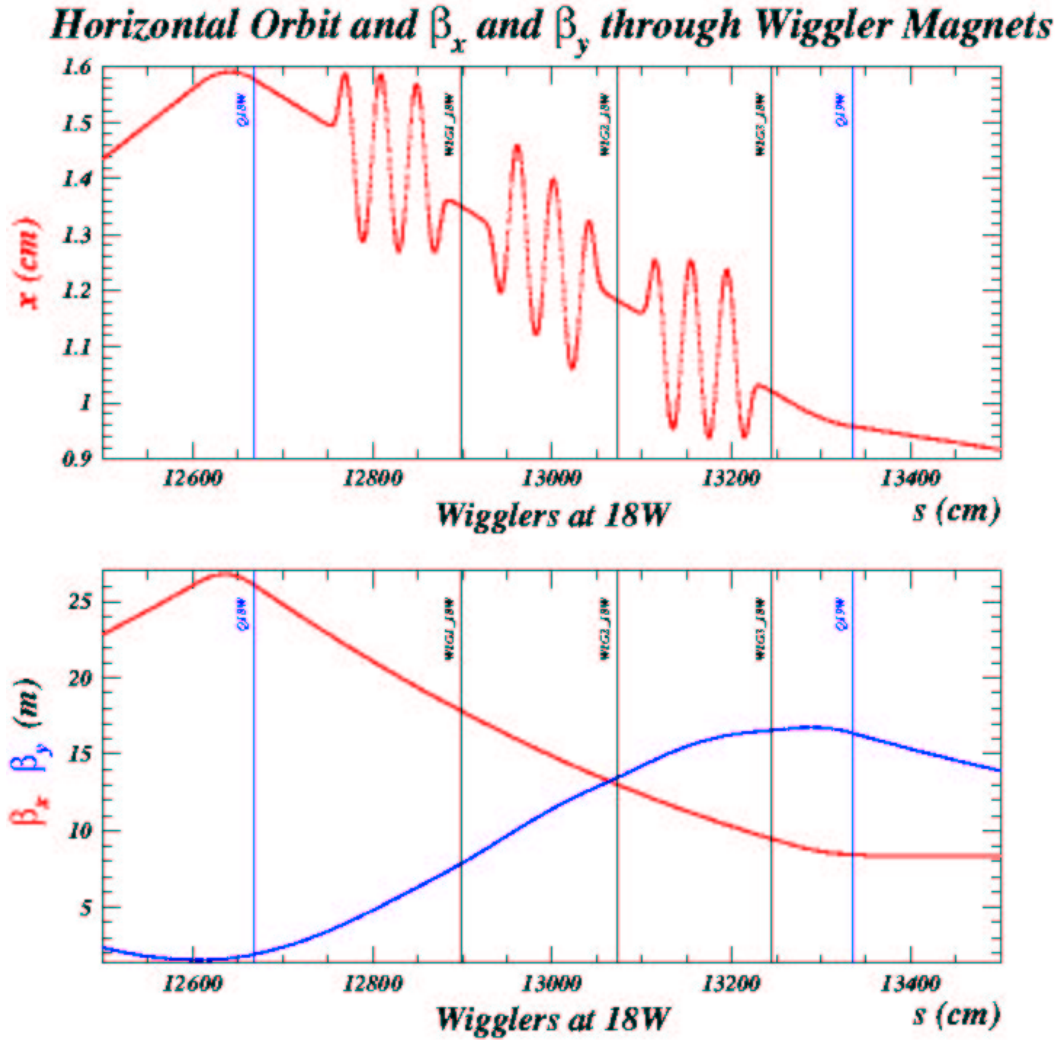


FIG. 9: Plots of the  $x$ ,  $\beta_x$  and  $\beta_y$  functions as they pass through the 3 wiggler magnets at position 18W.

can be concluded that wiggler magnets are slightly vertically focusing. An examination of the horizontal  $\beta$  function shows that the focusing effect of the wigglers is completely in the vertical direction and not at all horizontal.

Fig. 10 shows a more focused view of the interaction point, plotting 20 m on either side of it. It can be seen that the beam is roughly centered in the beampipe in both transverse directions, being less than 0.3 cm from the center of the pipe in either direction. Also, it can be seen that the beam enters the detector at a slight angle from the theoretical orbit. From the bottom graph, it still seems as though the  $\beta$  functions approach a value close to zero at the IP. A closer view is required to see exactly how big the  $\beta$ 's are at the IP.

Fig. 11 shows an even more focused plot of the IP, plotting only 2 cm on either side. It is clear that the  $\beta$  functions do not go to zero, but have concrete values. The horizontal  $\beta$  function averages about 84 cm, while the vertical  $\beta$  function averages about 1 cm. This strong focusing is achieved by employing very strong quadrupoles, just before and after the IP. In addition to looking at conditions in the beam while tracking once around the ring,

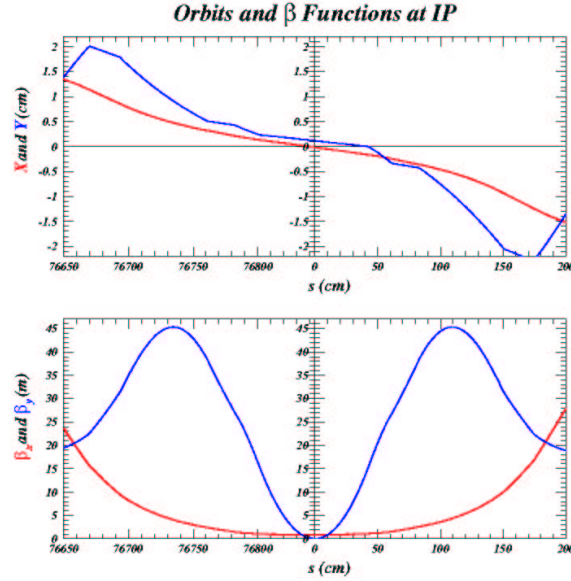


FIG. 10: Plot of the  $x$  and  $y$  orbits and the  $\beta_x$  and  $\beta_y$  functions as they cross the IP.

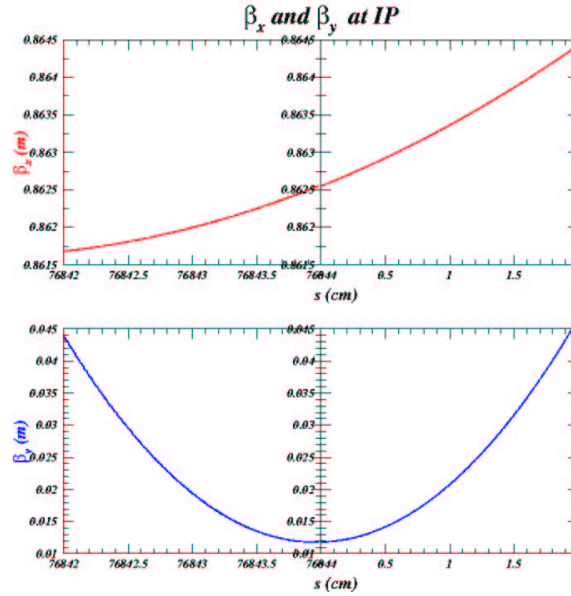


FIG. 11: Close up view of the  $x$  and  $y$  orbits and the  $\beta_x$  and  $\beta_y$  functions as they cross the IP.

studies were conducted to see how the bunch current and the pretzel orbit amplitude affected the  $\beta$  functions.

Fig. 12 shows a section of the ring and the  $\beta_x$  function as the bunch current in the opposing beam is varied from 0 mA to 2.5 mA. The left face of the graph in a way represents the two-dimensional plots of the  $\beta_x$  function as seen in Fig. 8. A small piece of the ring, from  $s = 700$  m to  $s = 740$  m, was sliced out from the plot and focused in on in order to show individual undulations in  $\beta_x$ . This  $\beta$  function was then plotted again, changing to higher

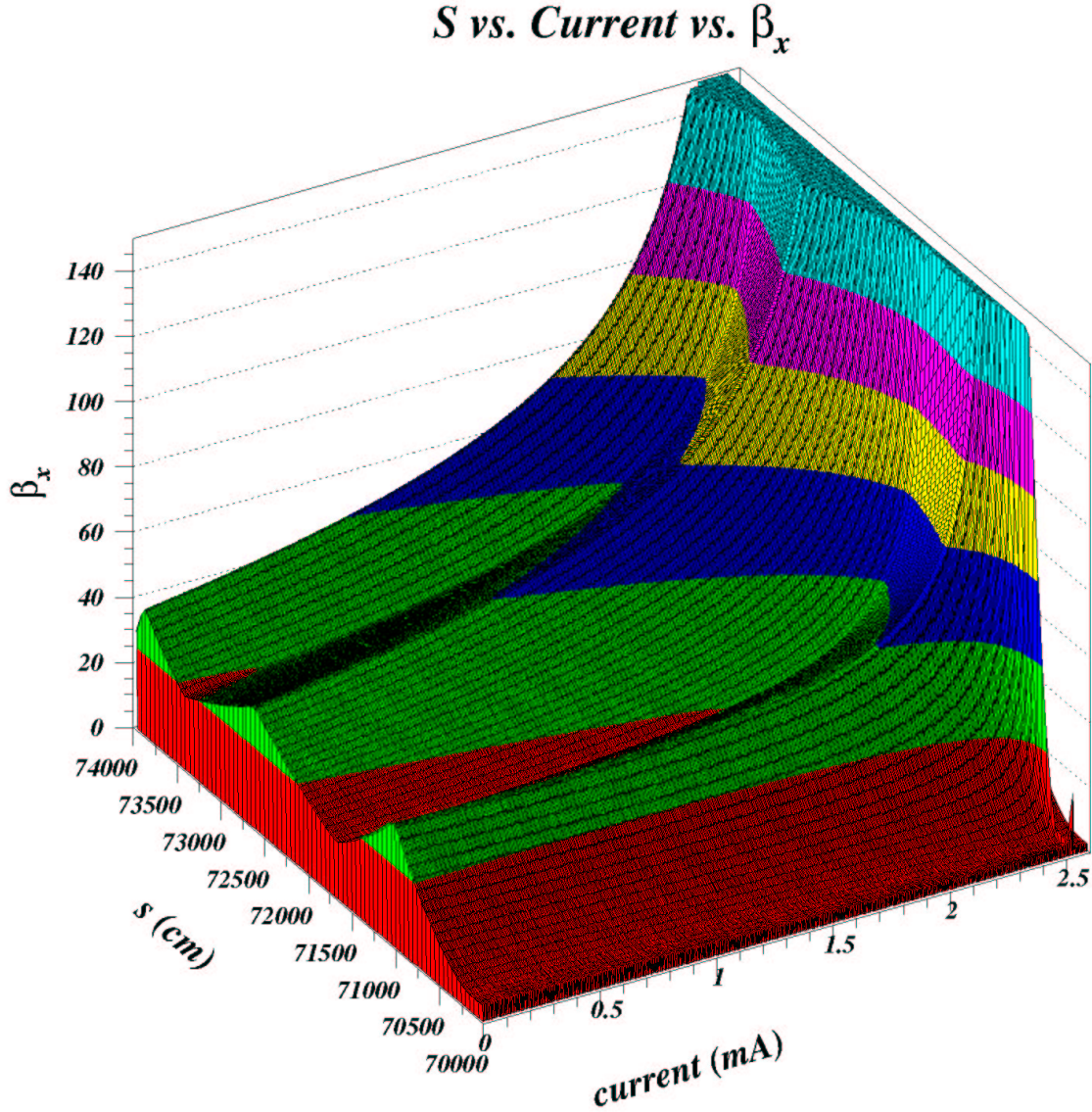


FIG. 12: Plot of the change in the  $\beta_x$  function around the entire ring as a function of the current in each beam bunch of the second beam. Note the spike at current  $\approx 2.5$  mA.

and higher values of the electron beam current. The most noticeable feature of this graph is the spike in the  $\beta$  function when current is approximately 2.5 mA. Since the  $\beta$  function corresponds to the size of the beam, a spike in it implies that the beam has inflated to such a size that it has blown itself completely out of the beampipe. Obviously, such resonances are to be strictly avoided when designing and tuning an accelerator. To understand what causes this spike to occur, we must examine Fig. 13.

The first graph in Fig. 13 shows the maximum value of  $\beta_x$  plotted against the current in the other beam. We see that this corresponds to a view of Fig. 12 from its right side. This dependence of the  $\beta$  function on the bunch current is a consequence of the beam beam interactions. If the code is run with identical settings and the LRBBI and IPBBI turned off, the  $\beta$  function shows absolutely no current dependence. As the particle beam sees more and

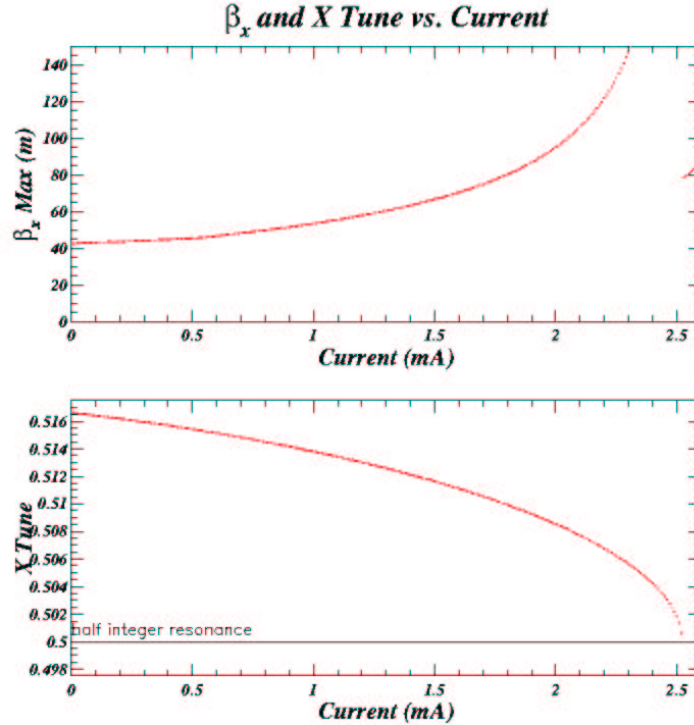


FIG. 13: The top graph is a side view of Fig. 12 showing the spikes in the  $\beta_x$  function. The lower graph is a plot of the  $x$  tune value during the same run. The spike corresponds to the point at which the  $x$  tune reaches the half integer resonance.

more current in the opposing beam, it's  $x$  tune decreases. This is because the LRBBI have a defocusing effect. As the bunches interact through the Coulomb force, they tend to spread each other out in space. The wider the beam becomes, the less effectively the quadrupoles can refocus it. Eventually the tune will hit a resonance and the beam will be lost. The lower graphs shows the values of the  $x$  tune for each data point in the upper graph. As the focusing slips, the tune decreases because the quadrupoles cannot force the beam into as many oscillations in one turn around the ring. We see that just at the point where the  $\beta$  function spikes, the value of the  $x$  tune approaches 0.5. It can be concluded from all this information that, with the current lattice, no values of bunch current near 2.5 mA will result in a stable particle orbit due to the half integer tune resonance.

Fig. 14 is very similar to Fig. 12 in its purpose and outcome. It represents two of the same variables as the graph in the previous section. The difference is that this time, instead of iterating over bunch current, it iterates over values of the pretzel orbit amplitude. It is obvious to see that there is a spike in the  $\beta_x$  function around  $\text{prz13} = 1500$ . As before, the tunes must be examined to fully understand this phenomenon.

Fig. 15 is analogous to Fig. 13 in its purpose. The only difference is what's being plotted on the  $x$  axis. In the top plot, we see a view of the right side of Fig. 14. It's easy to see the single spike. The lower plot shows that, as expected, the spike in the  $\beta$  function corresponds to a point at which the  $x$  tune is equal to a half integer. From this information it can be concluded that with a bunch current of 2 mA, which is the setting for this run, pretzel values near 1500 will cause an instability and should be avoided.

### *S vs. Pretzel Amplitude vs. $\beta_x$*

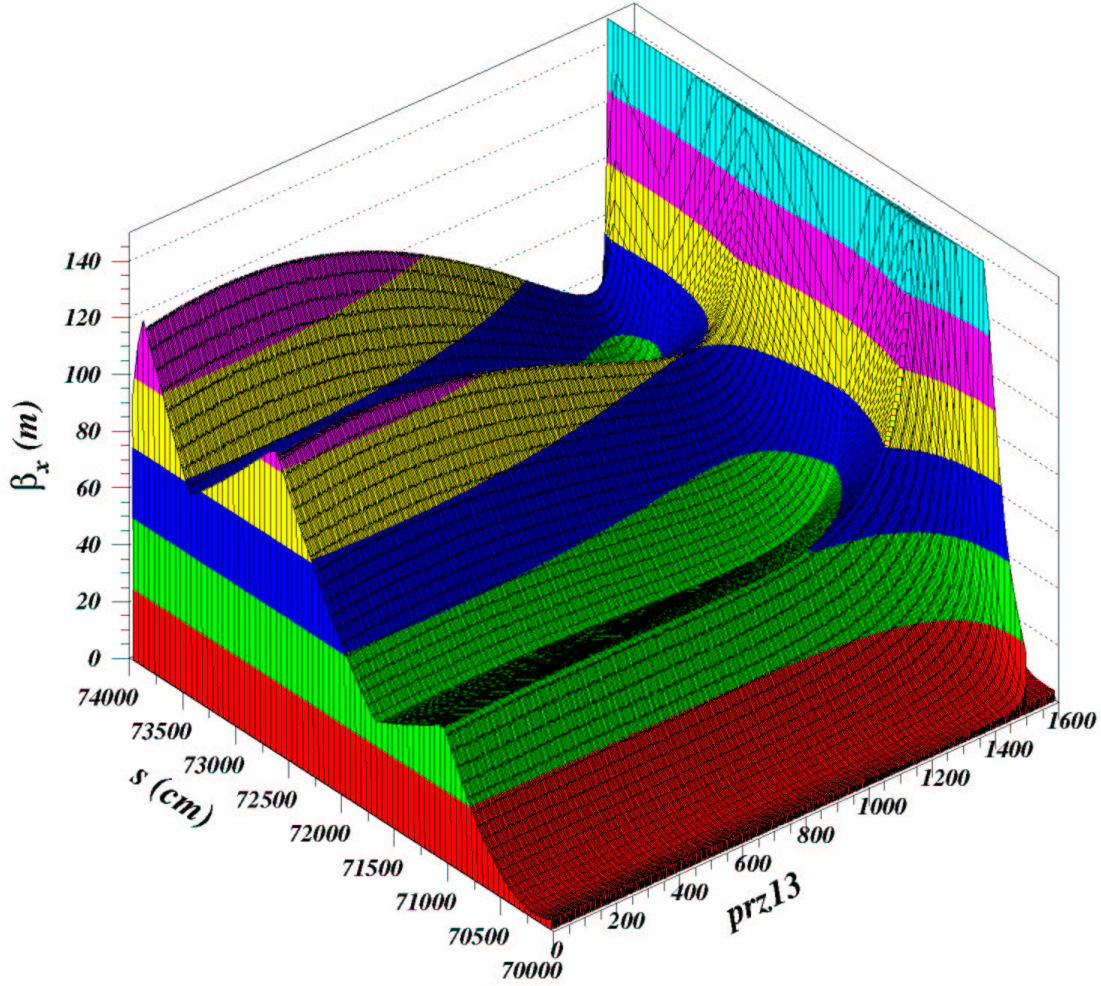


FIG. 14: Plot of the change in the  $\beta_x$  function around the entire as a function of the amplitude of the pretzel orbit. Note the spike at  $\text{prz13} \approx 1500$ .

## V. CONCLUSION

Using the computer simulations developed over this summer, the properties of the current 1.8 GeV lattice being used for CESR-c were analyzed. The properties of both the individual components of the lattice and the lattice as a whole were examined. The characteristics of the accelerator that were encountered were explained through a basic knowledge of accelerator physics. Also, points of instability were found in the settings for the bunch current and the pretzel orbit amplitude.

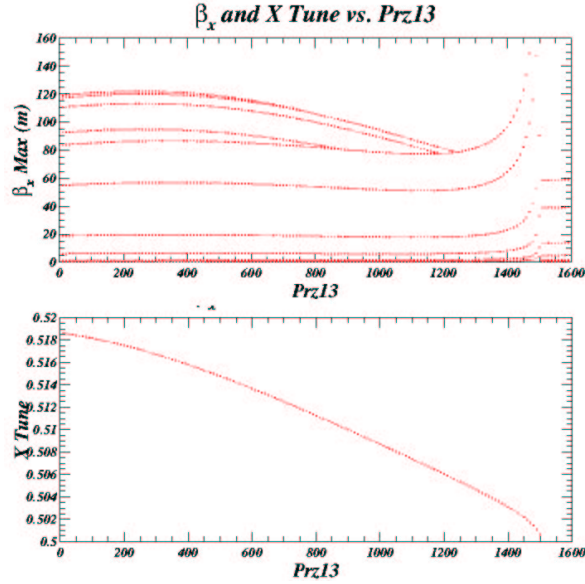


FIG. 15: The top graph again is a side view of Fig. 14 showing the spikes in the  $\beta_x$  function. The lower graph is a plot of the  $x$  tune value during the same run. The spike again corresponds to the point at which the  $x$  tune reaches the half integer resonance.

## VI. ACKNOWLEDGEMENTS

The author would like to thank his mentor, Dr. Jim Crittenden, for all of his guidance and helpful suggestions. Thanks also to Mr. David Kettler, who provided daily technical assistance in learning Linux, Fortran, and PAW. Also thanks to all the other REU students for creating a fun environment in which to live and work. Additionally, thanks go to Dr. Rich Galik and all those who helped organize this wonderful program. Finally, supreme thanks go to the National Science Foundation for their financial and organizational assistance. This work was supported by the National Science Foundation REU grant PHY-0243687 and research cooperative agreement PHY-9809799.

- 
- [1] Edwards, D.A. and Syphers, M.J.  
 An Introduction to the Physics of High Energy Accelerators  
 John Wiley and Sons: New York, 1993